Numerical simulation of icing effects on static flow field around blade airfoil for vertical axis wind turbine

Li Yan[1], Chi Yuan[1], Han Yongjun[1], Li Shengmao[1], Tagawa Kotaro[2]

(1. *College of Engineering*, *Northeast Agricultural University*, *Harbin*, 150030, *China*;

2. *Faculty of Regional Sciences*, *Tottori University*, *Tottori*, 6808552, *Japan*)

Abstract: Icing on blade surface of the straight-bladed vertical axis wind turbine (SB-VAWT) set in cold regions is a serious problem.   To study the performance effects of icing on SB-VAWT, numerical simulations were carried out on the ice accretion on NACA 0015 airfoil which was always used for blade airfoil of SB-VAWT by CFD methods based on 2D steady incompressible N-S Equation.   The morphology and procedure of icing on blade airfoil were obtained under different wind speeds, attack angles of blade and water flow flux in wind.   The static flow fields, especially the static pressure fields around blade airfoil with or without icing on it were computed.   The aerodynamic characteristics including the lift and drag force coefficients of blade airfoil were also calculated.   The results indicated that icing caused the static pressure field changed greatly and led to the increasing of drag force and reducing the aerodynamic performance.

Keywords: vertical axis wind turbine (VAWT), icing, blade airfoil, static flow field, numerical simulation

DOI: 10.3965/j.issn.1934-6344.2011.03.041-047

1   Introduction

For the wind turbines installed in cold regions, the icing on blade surface is a serious problem, for it will cause some negative effects on wind turbine performance, such as changing the load on blade, affecting the aerodynamics forces, and reducing the torque and power output, etc[1].   Therefore, people have done a lot of research work on wind turbine icing problem, among

them most researches focused on the Horizontal-axis Wind Turbine (HAWT) as it is the most popular type[2-5].   However, the Vertical-axis Wind Turbine (VAWT), especially the Straight-bladed VAWT (SB-VAWT) becomes popular for the use of small scale wind energy system recently.   The SB-VAWT is a kind of lift type VAWT (see Figure 1).   It has the main advantages of simple design, low cost and good efficiency.   However, it is affected by icing problem too[6].   Authors have done some researches of the icing effects on the SB-VAWT[7,8].   In this study, numerical simulations were carried out on the icing effects on a blade profile with NACA0015 airfoil which was always used by the SB-VAWT.   The simulation focused on the static flow fields around the blade with or without icing because the starting performance of SB-VAWT is dependent on the rotor azimuth angle against wind[9,10].   The dynamic performance simulation will be carried out in the future. The simulation conditions such as wind speed, water flow flux in wind were based on the outside experiment

results[7].   The pressure fields around blade were calculated and the aerodynamic force including lift force and drag force were also obtained.   Based on these results, the icing effects on the static performance of the blade profile were discussed.
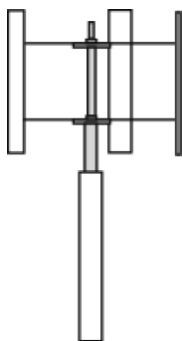
Figure 1   The SB-VAWT

2   Methods

2.1   Numerical simulation for icing

NACA series airfoils are always used for the blade airfoil for the SB-VAWT, such as NACA0012, NACA 0015 and NACA 0018.   Therefore, the NACA0015 airfoil was selected as the blade aerofoil for numerical simulation.   Considering that the wind tunnel test will be carried out in the future for comparison with the simulation results and the outlet size of wind tunnel we have is 1 m×1 m, the blade chord for computation was decided as 0.3 m.   The flow field was 3 m×3.3 m area which was shown in Figure 2.   The triangular mesh grids were provided for computation, and the model was discretized into approximately 30 000 elements (see Figure 3).
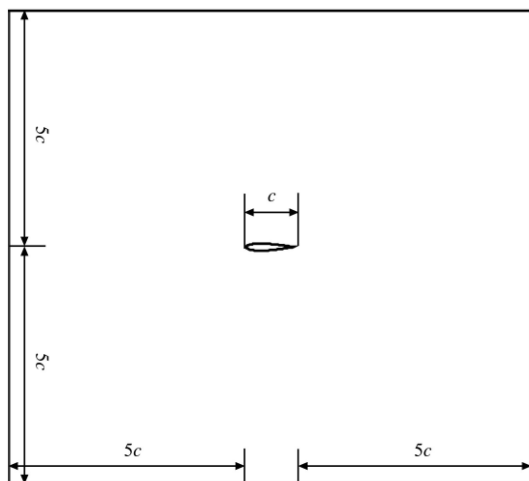
Figure 2   Flow field for the simulation
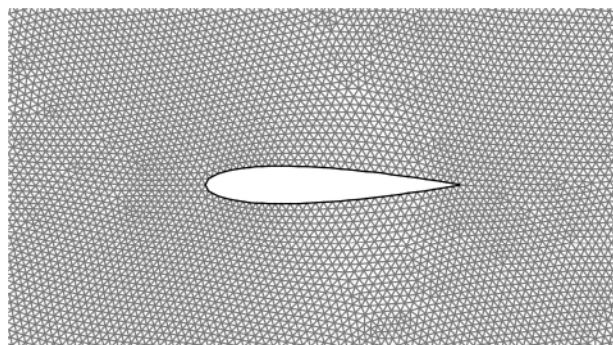
Figure 3   Grid mesh around the blade

The wind speeds for computation were designed as 4 m/s, 6 m/s and 8 m/s to make a comparison of Reynolds number.   The water flow fluxes flowing with wind which can be represented as the humidity of air were set as two types: 0.5 L/min and 1 L/min.   The temperature was ranged from 0° to -6°. To compare the effects of attack angle (α) of the blade, four attack angles were selected: 0°, 15°, 30° and 180°.   The definition of attack angle was shown in Figure 4.
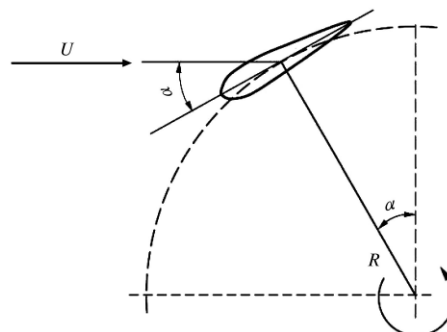
Figure 4   Definition of the attack angle of the blade

2.2   Mathematical model

The simulation for the original blade airfoil used the k-ε turbulence model, and a discrete phase model (DPM) was added to simulate the icing procedure.   Considering of the conservation of the mass, momentum and energy, the integral expression of the N-S equation in 2 dimensions incompressible steady flow is:

$$\frac{\partial}{\partial_t}\int_\Omega Wd\Omega + \int_s Fnds = \frac{1}{\text{Re}}\int_s F_v nds \qquad (1)$$

Where, Ω is a random unit; s is the boundary; W is the conservation variable; F represents non-viscous flux; F_v represents the viscidity flux; n is the unit normal vector and Re is the Reynolds number.

According to the conditions in the computation, the

continuity equation and momentum equation were shown as below:

$$\frac{\partial \rho}{\partial t} + \frac{\partial (\rho u_j)}{\partial x_j} = 0 \qquad (2)$$

$$\frac{\partial (\rho u_i)}{\partial t} + \frac{\partial (\rho u_i u_j)}{\partial x_j} = \frac{\partial \left[\mu_e \left(\frac{\partial u_i}{\partial x_j} + \frac{\partial u_j}{\partial x_i} \right) \right]}{\partial x_j} - \frac{\partial P}{\partial x_i} + S_i \qquad (3)$$

Where, ρ is the fluid density, kg/m^3; x_j is coordinate component; $u_i u_j$ is average relative velocity components; μ_e is significant viscosity coefficient; P is pressure, Pa; S_i is generated item.

Because the simulation was based on a two dimensions flow and the particles were very tiny, the Saffman lift was ignored[5]. The DPM control equation could be expressed as follows:

$$m_d \frac{du_d}{dt} = \frac{1}{2} \rho_a A_d C_d |u - u_d|(u - u_d) + m_d g \qquad (4)$$

Where, m_d is quality of the particle, kg; ρ_a is density of particle, kg/m^2; C_d is drag coefficient; u is wind speed, m/s; u_d represents particle velocity, m/s; A_d represents upwind area, m^2. Then the equation can be reduced as:

$$du_d / dt = f(u - u_d)/\tau + g \qquad (5)$$

The tracks of the water particles can be obtained from the water particles velocity integral.

3 Results and discussion

Based on the methods introduced above, the icing distributions on blade airfoil surface were computed. The static pressure fields around the original airfoil and iced airfoil were calculated. Furthermore, the lift and drag force coefficients were also obtained and the aerodynamic performance were discussed.

3.1 Pressure fields analysis

Figures 5 to 7 show the comparisons of static pressure fields around the original airfoil and iced airfoil under different affecting factors including wind speed, water flow flux in wind and attack angle of airfoil. The simulation results are expressed in the form of pressure contour map.

Original blade   Iced blade
a. $\alpha = 0°$

Original blade   Iced blade
b. $\alpha = 180°$

Original blade   Iced blade
c. $\alpha = 15°$

Original blade   Iced blade
d. $\alpha = 30°$

High pressure   Low pressure
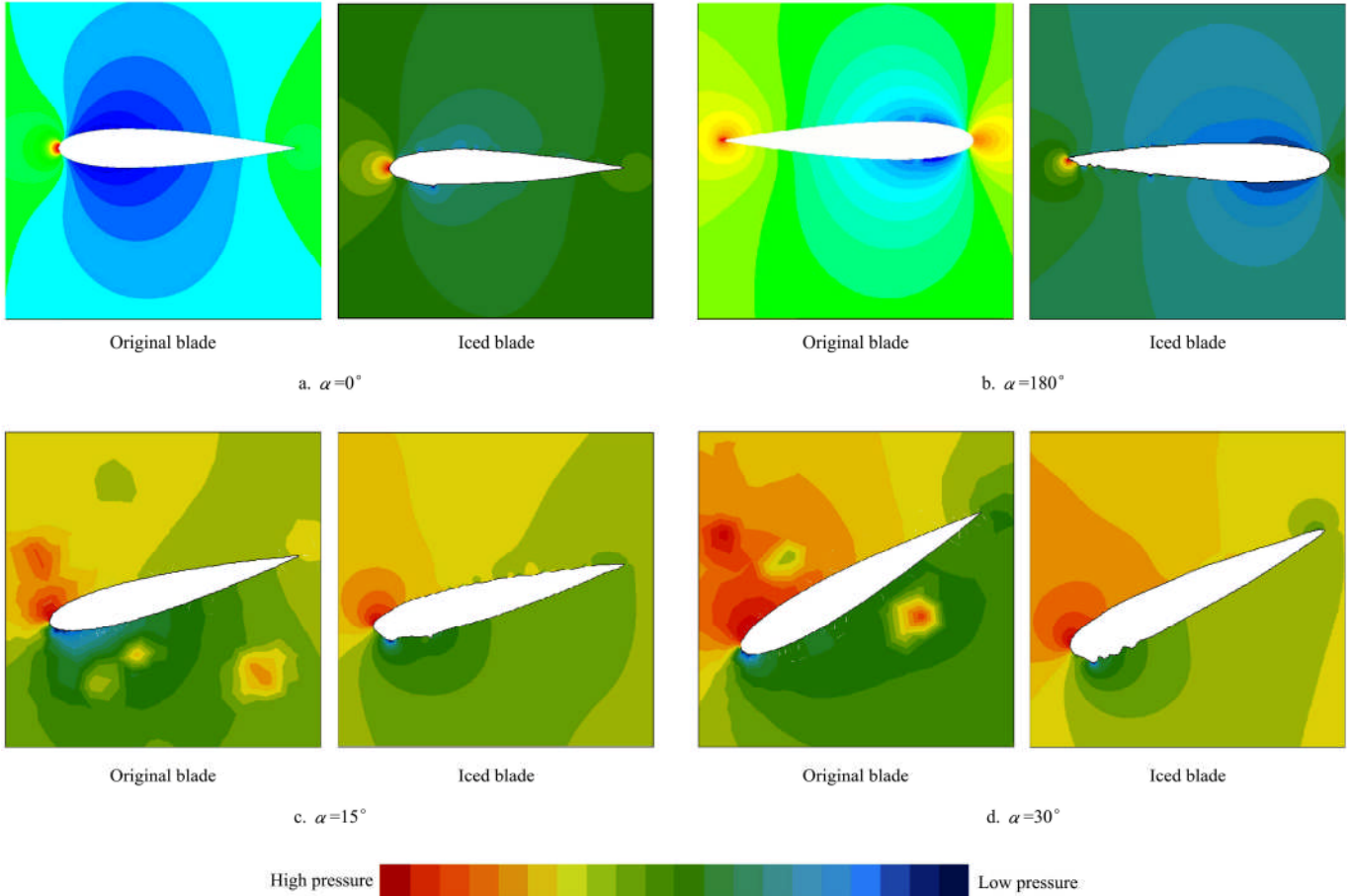
Figure 5   Pressure contours for the original blade and iced blade at different attack angles

a. $\alpha=0°$, $U=4$ m/s

b. $\alpha=0°$, $U=8$ m/s

c. $\alpha=180°$, $U=4$ m/s

d. $\alpha=180°$, $U=8$ m/s

High pressure ▬▬▬▬▬▬▬▬▬▬▬ Low pressure
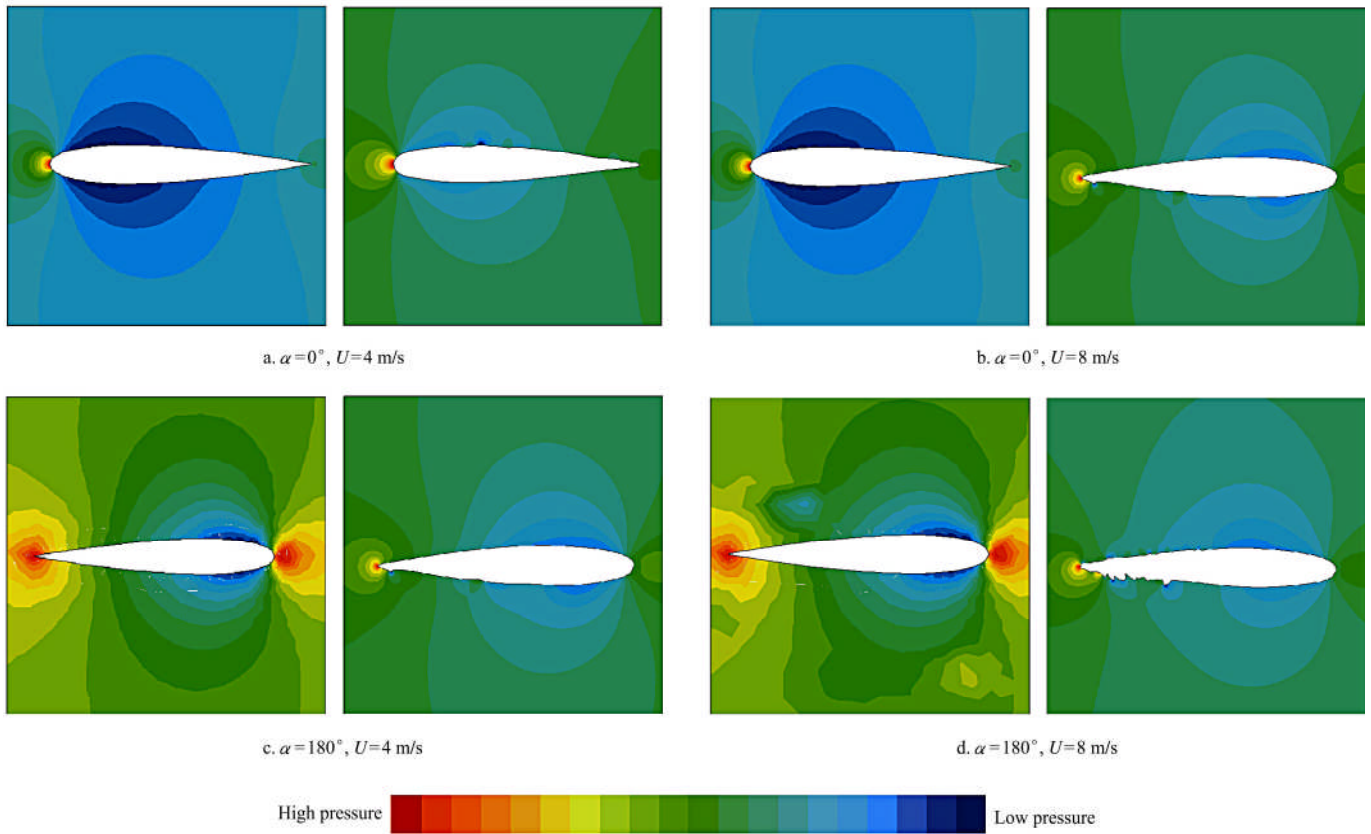
Figure 6   Pressure contours for the original blade and iced blade at different wind speeds

a. Original blade ($\alpha=15°$, $U=8$ m/s)

b. Iced blade ($\alpha=15°$, $U=8$ m/s, $Q=0.5$ L/min)

c. Iced blade ($\alpha=15°$, $U=8$ m/s, $Q=1$ L/min)

d. Iced blade ($\alpha=30°$, $U=8$ m/s)

e. Iced blade ($\alpha=30°$, $U=8$ m/s, $Q=0.5$ L/min)

f. Iced blade ($\alpha=30°$, $U=8$ m/s, $Q=1$ L/min)

High pressure ▬▬▬▬▬▬▬▬▬▬▬ Low pressure
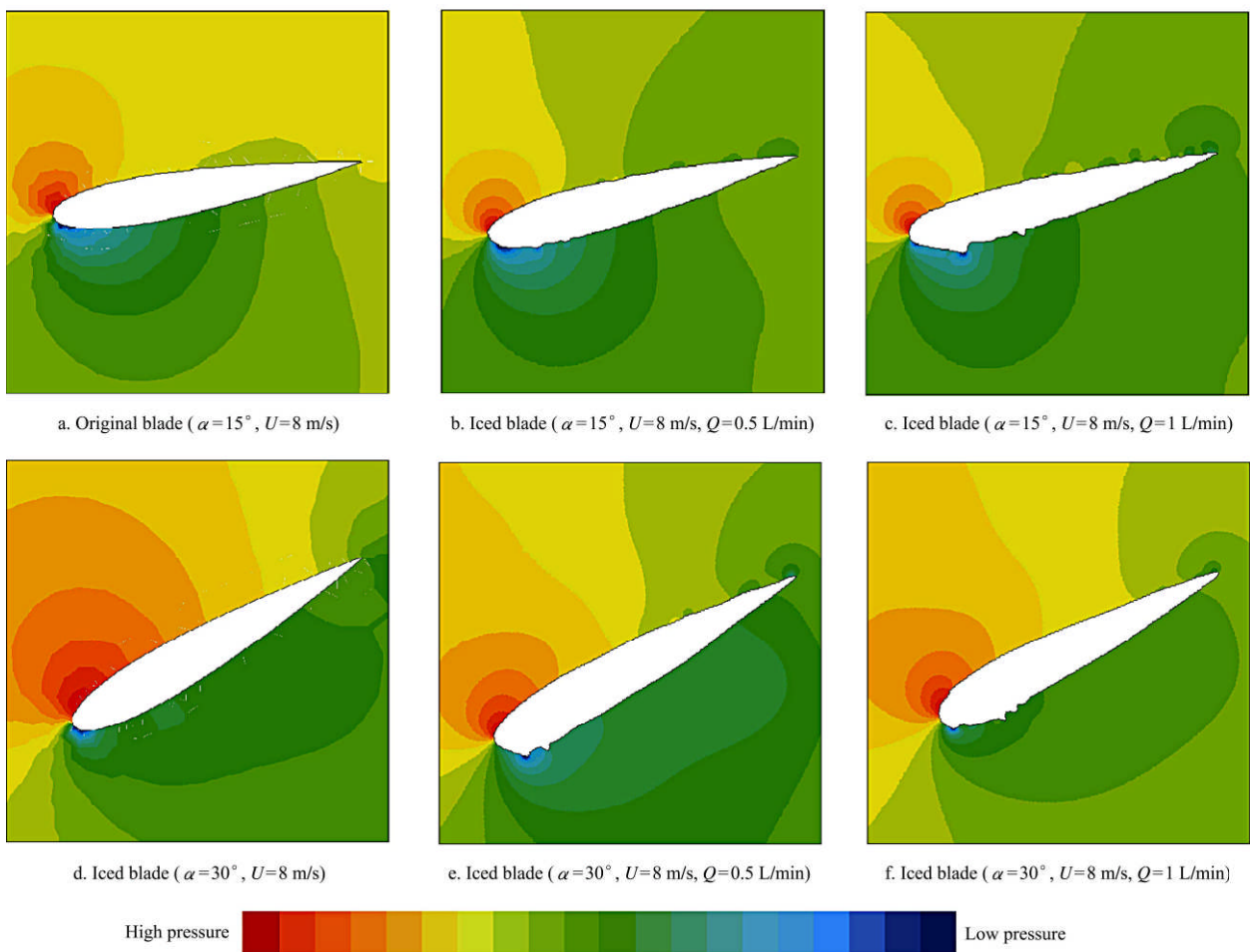
Figure 7   Pressure contours for the original blade and iced blade at different water flow flux

Figure 5 shows the pressure fields of the original blade and iced blade at different attack angles under the wind speed of 6 m/s and the water flow flux of 1 L/min. It can be seen that the pressure fields around the blade with or without icing are quite different at the same attack angle. The larger attack angle can increase the wind blow area for the blade and high pressure area, which works for both original and iced blade. The pressure gradient of iced blade is smaller than that of original blade. The icing amount on the down side of blade surface is larger than the up side, which shows the pressure changing effects on the icing on blade. The increasing of pressure will lead to more ice accretion on blade.

Figure 6 shows the wind speed effects on pressure fields of the original blade and iced blade at the attack angles 0° and 180° and water flow flux of 1 L/min. It can be seen that there is a high pressure area in the leading-edge of the original and icing blade, however the high pressure area for the iced blade is larger than that for the original blade. It shows that the leading-edge is easier to icing, which will change the shape of the blade and the aerodynamic characteristics. Although the blade airfoil is symmetrical, the icing on both sides of blade surface and the pressure fields around blade are dissymmetrical. The icing on blade surface changes the symmetrical airfoil and then makes the flow fields changed. Therefore, the pressure field changes and affects the icing on blade again, which is the reason of icing accretions on blade. According to Figure 6, with the increasing of wind speed, the icing on blade increases both for the attack angles 0° and 180°, and the pressure field changes greatly.

Figure 7 shows the water flow flux effects on pressure fields of the original blade and iced blade at the attack angles 15° and 30° and wind speed of 8 m/s. The larger water flow flux makes the blade to get more ice accretion on it and changes the shape much more than that at small water flow flux. This causes low pressure areas especially at the leading-edge and down side of blade airfoil.

3.2 Aerodynamic characteristics analysis

Figure 8 shows the lift and drag force coefficients that can express the aerodynamic performance of blade airfoil under the simulation conditions. The drag force and the lift force were obtained from the computation and then the lift and drag force coefficients can be calculated by the formulas shown as follows:

$$C_l = \frac{L}{\frac{1}{2}\rho A V^2} \tag{6}$$

$$C_d = \frac{D}{\frac{1}{2}\rho A V^2} \tag{7}$$

Where, V is the wind speed, m/s; A is the sectional area of the blade, m^2; L is the lift force, N; D is the drag force, N.

For the drag force, the icing on blade airfoil makes the drag force increased greatly comparing with the original blade without icing for all the cases. Usually, the drag force becomes larger with the increase of wind speed and water flow flux. For the attack angle of 180°, even the direction of drag changed. For the lift force, the icing on blade also changed the lift force. However, the degrees of change were different with the attack angle, wind speed and flow flux. And the lift force did not change as much as the drag force.

Furthermore, according to the ratio of lift and drag force defined as the ration of lift force and drag force which is another key factor for the aerodynamics performance of SB-VAWT, it can be also found that the performance of iced blade airfoil greatly reduced. For example, at the attack angle of 30° and wind speed of 6 m/s, although the lift coefficient just changed from -0.86 to -0.82, the ratio of lift and drag was changed from 1.5 to 0.85 which indicates that the blade aerodynamic performance becomes poor.
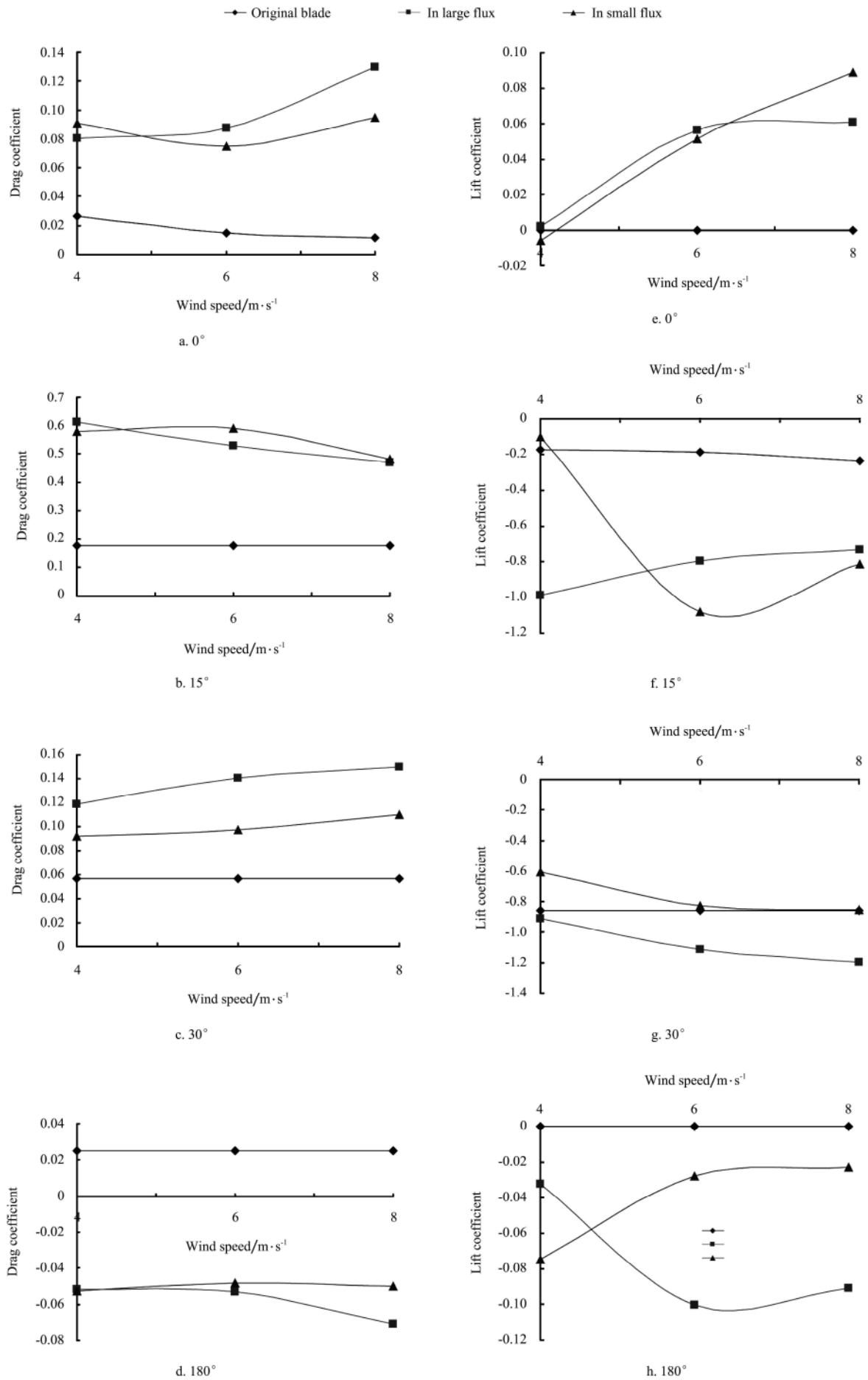
Figure 8   Lift and drag force coefficients

4   Conclusions

The simulations of the static aerodynamic performance effects on the original and icing blade airfoil were carried out in this study.   The pressure field contours around the blade airfoil and the aerodynamics forces were obtained.   The conclusions can be summarized as follows under the simulation conditions in this study:

1) The water flow flux and wind speed are the two main factors which affect the icing and ice accretion on blade airfoil.   With the increase of wind speed and water flow flux in wind, the ice accretions increased generally.

2) The icing accretion and distributions on blade airfoil are quite different at different attack angles of blade airfoil. Although the icing condition has no obvious rule, the icing amount becomes more at the attack angel which the blade has large projected area.

3) Icing on the symmetrical blade airfoil at the angle of 0° and 180° can change the airfoil to dissymmetrical shape, which causes the pressure field changed and leads to the increase of drag force and decrease of the aerodynamics performance.

4) Icing on blade airfoil makes the drag force increase greatly which leads to the ratio of lift and drag force reduced.   The blade performance becomes poor.

Acknowledgments

[References]

[1]   Nalili N, Edrisy A, Carriveau R.   A review of surface engineering issues critical to wind turbine performance.   Renewable and Sustainable Energy Reviews, 2009; 13: 428-438.

[2]   Neil Bose.   Icing on a small horizontal-axis wind turbine – Part 1: Glaze ice profiles.   Journal of Wind Engineering and Industrial Aerodynamics, 1992; 45: 75–85.

[3]   Neil Bose.   Icing on a small horizontal-axis wind turbine - Part 2: Three dimensional ice and wet snow formations.   Journal of Wind Engineering and Industrial Aerodynamics, 1992; 45: 87-96.

[4]   Makkonen L, Laakso T, Marjaniemi M. Modeling and prevention of ice accretion on wind turbines.   Wind Engineering, 2001; 25(1): 3-21.

[5]   Andrea G, Kraj, Eric L Bibeau.   Measurement method and results of ice adhesion force on the curved surface of a wind turbine blade.   Renewable Energy, 2010; 35: 741-746.

[6]   Yang Baisong, Li Yan, Feng Fang, Li Shengmao.   Observation and analysis of icing on the static blade of straight-bladed vertical axis wind turbine.   Renewable Energy Resources, 2009; 27(6): 20–23.

[7]   Li Shengmao, Li Yan.   Numerical simulation on icing of a blade aerofoil for vertical axis wind turbines.   Journal of Chinese Society of Power Engineering, 2011; 31(3): 214-219.

[8]   Yan Li, Kotaro Tagawa, Wei Liu.   Performance effects of attachment on blade on a straight-bladed vertical axis wind turbine.   Current Applied Physics, 2010; 10(2), S1: 335-338.

[9]   Islam M, Ting D S K, Fartaj A.   Aerodynamic models for Darrieus-type straight-bladed vertical axis wind turbines. Renewable and Sustainable Energy Reviews, 2008; 12(4): 1087-1109.

[10]   Seki K.   Research and development of high-performance airfoil sections for vertical axis wind turbine at low-Reynolds number.   Trans of JSME, 1991; 57(536): 1297-1304.